ELSEVIER

Journal of Photochemistry and Photobiology A: Chemistry 134 (2000) 87–95

Journal of Photochemistry and Photobiology A:Chemistry

www.elsevier.nl/locate/jphotochem

Fluorescence quenching mechanisms in micelles: the effect of high quencher concentration

D.T. Cramb*, S.C. Beck

Department of Chemistry, University of Calgary, 2500 University DR., Calgary, AB, Canada T2N 1N4

Received 10 January 2000; received in revised form 7 February 2000; accepted 14 February 2000

Abstract

In this investigation the fluorescence quenching of fluorescent probe molecules situated within surfactant micelles was examined. The hydrophobic polyaromatic hydrocarbon benzo(a)pyrene (B(a)P) and the more polar 6-propionyl-2-(dimethylamino)-naphthalene (PRODAN) were used to assess the effect of high quencher concentration on the quenching process in micelles. Using the surfactant systems sodium dodecyl sulfate (SDS) and Triton X-100 (TX-100), three distinct modalities of quenching were observed. For the TX-100 system, both I^- and H_2O_2 quenching of probe fluorescence reached saturation in efficiency. These data are modeled quite well by assuming a limited number of quenching sites per micelle in conjunction with standard Stern–Volmer quenching dynamics. For the SDS system, similar quenching saturation effects are observed, but the saturation model worked less well. It is suggested that a bimodal distribution of micelle sizes could be responsible. The B(a)P/SDS/I^- system is singular in that the quenching does not saturate. The efficiency of quenching here varies approximately with the third power of I^- concentration. A resonance energy transfer mechanism is proposed in which B(a)P is quenched by I_3^-.

Keywords: Fluorescence quenching; Micelles; Sodium dodecyl sulfate; Triton X-100

1. Introduction

Fluorescence quenching has been successfully exploited in the pursuit of understanding complex macromolecular systems both chemical and biological in nature. Extensive insight has been provided into the environment within micelles using steady state and time resolved fluorescence quenching [1–10]. The fundamental nature of micelle-mediated quenching has also been explored [11–18]. In the simplest scenario, quenching is modeled based on the Stern–Volmer [19] equation in which the ratio of fluorescence in the absence of quencher to that in the presence of quencher is a linear function of quencher concentration. Deviations from linearity generally fall into two categories: saturated and superlinear. In certain cases, the saturated behavior is characteristic of an inaccessible fraction of fluorophores [12]. This fraction is typically buried in a hydrophobic region of a macromolecular system, such as a protein. Indeed, in biology fluorescence quenching was first used to examine the positions of aromatic amino acids within proteins [20]. Moreover, high iodide concentrations have been employed in recent reports of tryotophan quenching for bovine serum albumin in the aqueous phase [21] and immobilized in a sol–gel [22]. Superlinear behavior is more common and usually occurs owing to a strong partitioning of the quencher into a region of space containing the fluorophore. Within micelle solutions, the kinetic equations for such behavior are based on the probabilities of finding the quenchers and fluorophores in the same micelle [23,24]. These probabilities are based on Poissonian micelle occupation statistics. A rarer, but simpler scenario for superlinear behavior is when both static and dynamic quenching occur simultaneously. This leads to a quadratic dependence on quencher concentration.

Recent reports of saturated fluorescence quenching in micelle/liposome solution include: the quenching of 6-propionyl-2-(dimethylamino)-naphthalene (PRODAN) by iodide ions in sodium dodecyl sulfate (SDS) micelles [25], the quenching of 2-aminonaphthaline and 2-aminochrysene by bromide ions in cetyltrimethylammonium chloride (CTAC) micelle solution [1] and for 6-fluoroquinolone–liposome interactions [26]. In the first study, the quenching was modeled as an inaccessible fraction, whereas in the second it was modeled based on a saturation of the bromide binding sites on CTAC micelles. The third study suggested that at high pH, coulombic repulsion was responsible for

* Corresponding author.
E-mail address: dcramb@ucalgary.ca (D.T. Cramb)

1010-6030/00/$ – see front matter
PII: S1010-6030(00)00249-5

a second type of quencher–probe interaction. The saturation was then accounted for in the Poisson analysis of ion binding. For all of these studies, the quencher concentration was considerable (0.1–0.5 M). In this situation, there may indeed be a saturation of micelles/liposomes by quenchers leading to nonlinear Stern–Volmer behavior. There is also the potential that at high ionic strength, a change in micelle size distribution could obfuscate the quenching data. Clearly, more studies are needed on high concentration quenching to determine whether or not there is a common mechanism for this process.

In this article, we have examined the quenching of fluorophores PRODAN and benzo(a)pyrene (B(a)P) in SDS and in Triton X-100 (TX-100) micelle solution. The quenchers used (iodide and peroxide) are employed in the concentration range where quenching saturation is expected to occur. For the iodide quenching we have kept the ionic strength constant by adding NaCl. In doing so we believe that the loss of fluorescence intensity occurs because of quenching and not due to changes in micelle structure. The fluorophores were chosen as examples of polar and nonpolar probes, which in principle will reside in different locations within a micelle. In addition to employing the modified Stern–Volmer equation for inaccessible fluorophores, we propose that quenching saturation results from a limited number of quenching sites per micelle. A saturation isotherm, analogous to a Langmuir adsorption isotherm used for modeling surface association phenomena [27], is employed. The model works very well for the TX-100 system and reasonably well for the SDS system. An interesting example of superlinear quenching behavior was observed in the case of B(a)P/SDS/I^-.

2. Experimental procedures

Stock solutions of fluorophores (10^{-3} M) were prepared in toluene. Aliquots of the stock solutions (100 μl) were micropipetted into brown glass bottles, the toluene removed with a stream of dry nitrogen and pH 6.7 (1 mM) phosphate buffer added (100 ml) to give 1 μM fluorophore solutions. Surfactant was added to give solutions of 1 mM micelle concentration. The solutions were sonicated for 15 min and allowed to equilibrate overnight. The critical micelle concentration for SDS is 8 mM and for TX-100 is around 0.2 mM.

Aliquots (5 ml) were placed in scintillation vials. Quencher and sodium chloride were added in varying concentrations to give a constant ionic strength of 0.4 mol kg^{-1}. The series of quencher concentrations were: 0.1, 0.2, 0.3, 0.35 and 0.4 M for NaI and 0.099, 0.195, 0.290, 0.336 and 0.382 M for H_2O_2. The solutions were again sonicated for 15 min and allowed to return to room temperature. Emission spectra were collected with a Photon Technology International LPS-220 spectrofluorimeter. Standard 1 cm quartz suprasil fluorescence cuvettes (Hellma) were used.

2.1. Chemicals

Benzo(a)pyrene was used as furnished by Dr. A. Okey (University of Toronto). Sodium iodide was purchased from BDH Inc. and was recrystallized from 9:1 (v/v) ethanol/water prior to use. All other chemicals were used as purchased: 30% H_2O_2 (aq) and NaCl (BDH Inc.), PRODAN (Molecular Probes), SDS and TX-100 (Sigma Chemical Co.).

3. Results

3.1. Fluorescence spectra

Steady state quenching experiments were performed using B(a)P or PRODAN as fluorescence probes and iodide ions or peroxide as the quencher. In Fig. 1a–c we display typical fluorescence spectra as functions quencher concentration. The spectral wavelength maxima were found to vary with added quencher (I^- or H_2O_2) only for the PRODAN/TX-100 system. It is informative to evaluate these spectra further. Here, there likely exists two different micellar sites for PRODAN, which results in the measured spectrum being a sum of two spectra. We speculate that only one of the sites may be accessible to the quencher. The result of increasing quencher concentration would be a systematic reduction of only one of the spectra. Thus, if one were to subtract the quencher-containing spectrum from quencher-free spectrum, one should observe the fluorescence spectrum of the accessible fraction. In Fig. 2, we show that this is the case for the PRODAN/TX-100/I^- system. The difference spectrum suggests that the accessible fraction has a peak near 490 nm. This is red-shifted with respect to the quencher-free spectrum and is indicative of the probe located in a more polar environment. Such an environment would be found near the micelle surface. However, the quenched peak is not at the same wavelength as PRODAN in pure H_2O (520 nm) [28]. Time resolved fluorescence measurements would help considerably to confirm our suggestions about fluorescence probe location, but are beyond the scope of the present work.

3.2. Quenching models

The reduction in fluorescence was determined by modeling the observed spectrum with the unquenched spectrum multiplied by a reduction coefficient [28]. In all cases, the observed spectrum was reproduced accurately with this method and error on the reduction coefficient was less than 1%. In Fig. 1a and c we presented the spectra for B(a)P and PRODAN, respectively, in TX-100 and SDS micelle solutions. The series represents a range of sodium iodide or H_2O_2 concentrations from 0.1 to 0.4 M. Recall that the ionic strength of the buffer solution was kept constant using NaCl so that the surfactant critical micelle concentration would remain constant. For aromatic systems, Cl^- ions

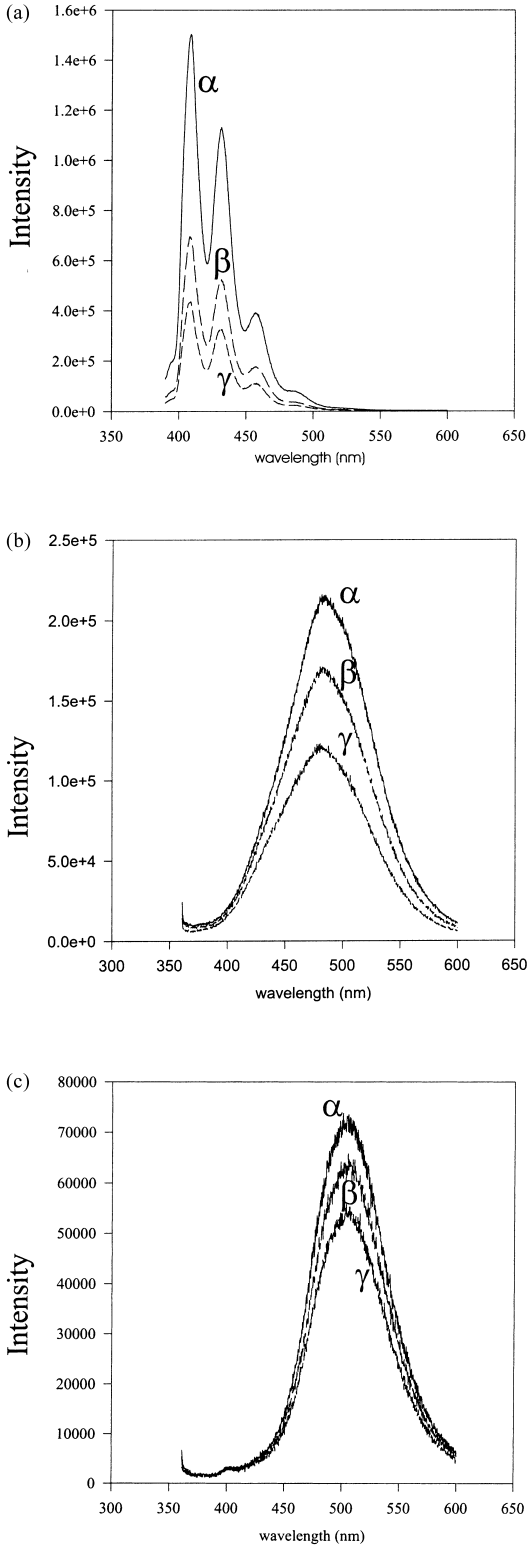

Fig. 1. Fluorescence spectra of (a) 1 μM benzo(a)pyrene excited at 380 nm and (b) and (c) 1 μM PRODAN, excited at 360 nm. In panel (a) B(a)P is solubilized in 2.5 mM TX-100 micelle solution and is quenched by I^-. In panel (b) PRODAN is solubilized in 2.5 mM TX-100 micelle solution and is quenched by I^-. In panel (c) PRODAN P is solubilized in 80 mM SDS micelle solution and is quenched by H_2O_2. The solvent in all cases is pH 6.7 phosphate buffer. The spectra are labeled as α, β or γ to indicate 0.0, 0.1 and 0.4 M, respectively, of the quencher indicated.

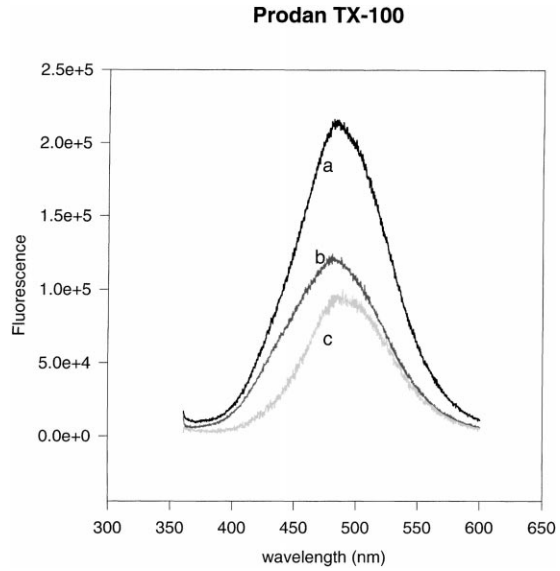

Fig. 2. The mathematical difference fluorescence spectra (c) of PRODAN in TX-100 between unquenched (a) and quenched by 0.4 M iodide (b). The excitation wavelength was 360 nm.

have been observed to quench fluorescence with nearly 1000-fold lower efficiency than I^- ions [16].

The simplest method for modeling the quenching phenomena is to use the Stern–Volmer approach

$$\frac{F_0}{F} = 1 + K_{SV}[Q], \tag{1}$$

where F and F_0 are the fluorescence intensity in the presence and absence, respectively, of quencher. K_{SV} is the Stern–Volmer constant and [Q] is the free quencher concentration. In the case of a large excess of quencher, the free and total quencher concentrations are taken to be equal. By using this simple Stern–Volmer equation, one assumes that there is a single type of quenching (static or dynamic) and that there is only one environment in which quenching takes place. Thus, a plot of F_0/F versus [Q] should yield a straight line with slope K_{SV}. Using this approach, our results were not modeled adequately. The best linear regression produced r^2 values of 0.94 for PRODAN in SDS quenched with H_2O_2. The chi-squared values from the non-linear least squares fits to the data are all near 0.05. The other datasets produced regression with r^2 values between 0.6 and 0.9. From Fig. 3, it is clear that in the case of the PRODAN/TX-100/I^- system there is a systematic deviation from the model. In every case, except that for B(a)P/SDS/I^-, the deviation from simple Stern–Volmer behavior results from a leveling off of the quenching at higher quencher concentration.

A saturation of quenching efficiency suggests that one or more of our initial assumptions about the quenching mechanism does not hold. The behavior described is typical of the scenario where fractions of the quencher and probe population are inaccessible to each other. If we consider a fraction of the probe molecules inaccessible, then a

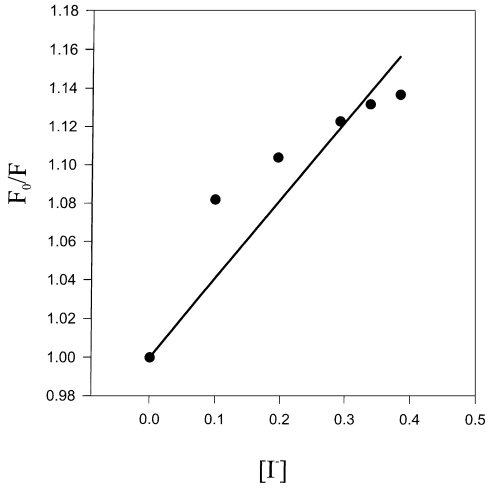

Fig. 3. Stern–Volmer plot of the fluorescence of 1 μM benzo(a)pyrene in 2.5 mM TX-100 micelle solution vs. iodide concentration (dots). The straight line is the best fit of the data to Eq. (1).

modified Stern–Volmer equation can be used to interpret the experimental results. This model can be written as [11]

$$\frac{F_0}{\Delta F} = \frac{1}{f_a K_{SV}[Q]} + \frac{1}{f_a}, \tag{2}$$

where $\Delta F = F_0 - F$ and f_a is the fraction of probe accessible to the quencher. Here a plot of $F_0/\Delta F$ versus l/[Q] should produce a straight line whose intercept provides f_a (as $1/f_a$) and whose slope provides K_{SV} (as $l/f_a K_{SV}$). We rearrange this equation in order to compare it with the site saturation model to be developed next.

$$\frac{F_0}{F} = \frac{1 + K_{SV}[Q]}{1 + f_b K_{SV}[Q]}. \tag{3}$$

In the above equation f_b is the fraction of inaccessible quencher. The saturation approach worked much better with r^2 values in the range 0.92–0.99. The chi-squared values here are around 0.0005. The results of this fit are shown in Table 1.

In the present work, Eq. (3) is only appropriate where one has spectroscopic evidence of different probe locations. As was shown above, this is true only for PRODAN in TX-100. Therefore, we will introduce another saturation mechanism. This is micelle quencher site saturation, rather than an inaccessible fraction of fluorescence probe. Therefore, we will present a formalism, which is different from previously developed [23,29]. In [29] the authors present saturation behavior based two different lipophilic sites for quencher partitioning, but where each site contains an active quencher. In our model we assume that there is only one type of quenching site and that it is saturable. Consider that for a quencher–probe encounter the standard Stern–Volmer equation applies. The trend toward a maximum in the quenching efficiency occurs because of the saturation of a finite number of micelle sites, *S*, from which quenching can occur. As the sites must be near the probe, *S* may be different for different fluorescence probes. It follows that at a quencher concentration below saturation, there will be some sites occupied and some sites unoccupied such that

$$[S]_T = [S]_{occ} + [S]_{free}, \tag{4a}$$

$$[Q]_T = [Q]_{occ} + [Q]_{free}. \tag{4b}$$

Therefore, the Stern–Volmer equation becomes

$$\frac{F_0}{F} = 1 + K_{SV}[Q]_{occ}. \tag{5}$$

The concentration of quencher occupying a quencher site within the micelle, $[Q]_{occ}$, can be estimated using an adsorption isotherm interpretation where the rates of quencher sites becoming free and occupied are

$$\frac{d[S]_{free}}{dt} = k_{off}[Q]_{occ} \tag{6}$$

and

$$\frac{d[S]_{occ}}{dt} = k_{on}[Q]_{free}[S]_{free}, \tag{7}$$

respectively. At equilibrium these rates will be equal. Therefore, we can combine Eqs. (4a), (6) and (7) and solve for $[Q]_{occ}$.

$$[Q]_{occ} = \frac{K_Q[Q]_{free}[S]_T}{1 + K_Q[Q]_{free}}, \tag{8}$$

where $K_Q = k_{on}/k_{off}$. Moreover, since $[Q]_{occ} = [S]_{occ}$ and since $[Q]_{free} \approx [Q]_T$ at high [Q] and low relative micelle concentration, we can rearrange Eq. (8) to give

$$[Q]_{occ} = \frac{[S]_T}{1 + (1/(K_Q[Q]_T))}. \tag{9}$$

We then substitute this result into Eq. (5) and rearrange to yield

$$\frac{F_0}{F} - 1 = \frac{K'_{SV}}{1 + (1/(K_Q[Q]_T))}, \tag{10}$$

where $K'_{SV} = K_{SV}[S]_T$. Thus, a plot of $F_0/F - 1$ versus $[Q]_T$ results in a line which asymptotically approaches K'_{SV} and

Table 1
The results of the chi-square fit

System	K_Q (M^{-1})	K'_{SV}
B(a)P/SDS/I^-	–	–
B(a)P/SDS/H_2O_2	9.1 (0.9)[a]	0.1 (0.06)
B(a)P/TX-100/I^-	19 (2)	0.82 (0.02)
B(a)P/TX-100/H_2O_2	4.8 (1.0)	0.12 (0.01)
PRODAN/SDS/I^-	2.8 (0.8)	0.30 (0.07)
PRODAN/SDS/H_2O_2	1.7 (1.0)	0.77 (0.4)
System	f_a	K_{SV} (M^{-1})
PRODAN/TX-100/I^-	0.68 (0.02)	4.32 (0.03)
PRODAN/TX-100/H_2O_2	0.15 (0.01)	10.62 (0.05)

[a] Numbers in parentheses indicate 1 S.D. in units of the value quoted.

from which the constant K_Q is available. Since we are using fluorescence quenching to measure the association of quenchers with micelles, both K_Q and $[S]_T$ will depend on the surfactant, the fluorescence probe and the quencher used. Not every quencher association site on the micelle may be ideal for the quenching process, therefore, $[S]_T$ will not be equal to the total number of micelle occupation sites. Eq. (10) is formally the same as Eq. (3), but the constants represent different phenomena.

Plots of the data versus that predicted using Eq. (10) are presented in Fig. 4a–d. The chi-squared values for the TX-100 micelles system are around 0.0005, whereas for the SDS system the chi-squared values are 0.003. The resulting constants derived from the fit to Eq. (10) can be found in Table 1.

For completeness, we must also consider that it may be possible to model the saturation of quenching using Poisson statistics of micelle occupation. If the quencher–probe pair

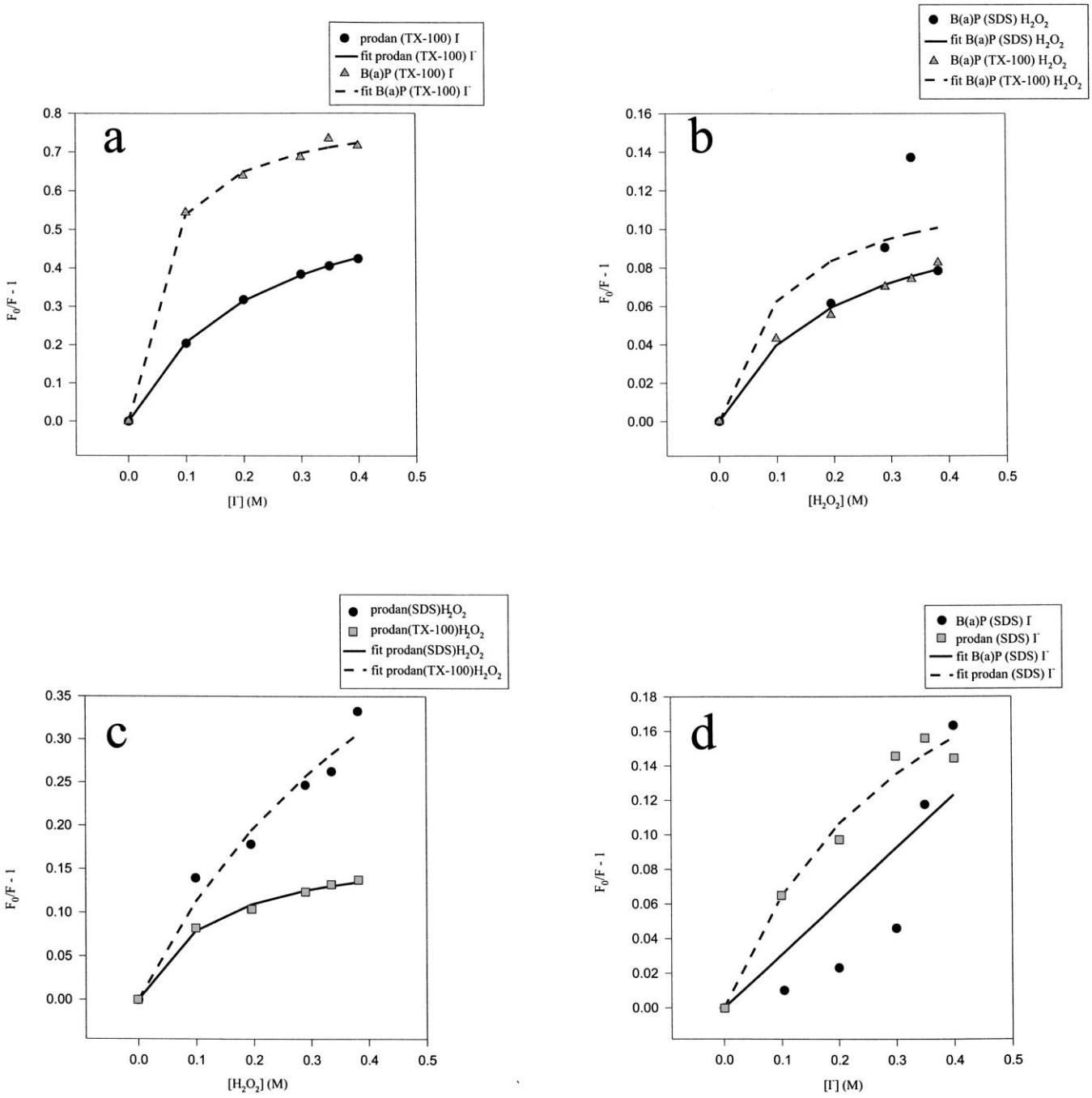

Fig. 4. Stern–Volmer plots of the fluorescence of 1 μM benzo(a)pyrene and PRODAN for all micelle solutions. The lines are the best fits of the data to Eq. (10). See insets for details of the solutions plotted.

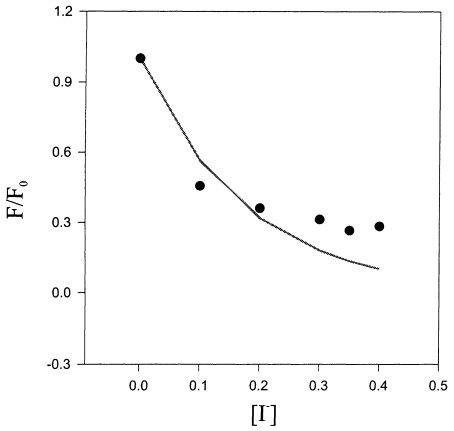

Fig. 5. Plot of the fluorescence quenching of 1 μM benzo(a)pyrene in 80 mM SDS micelle solution by iodide ions. The line is the best fit of the data using Eq. (11).

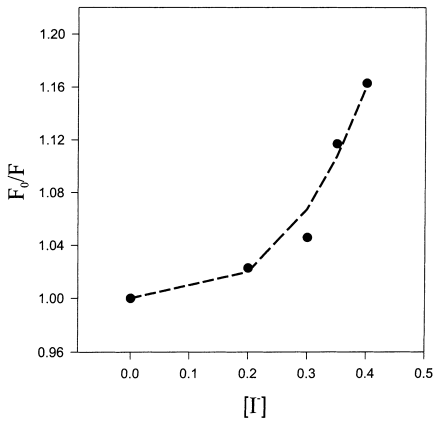

Fig. 6. Plot of the fluorescence quenching of 1 μM benzo(a)pyrene in 80 mM SDS micelle solution by iodide ions. The line is the best fit of the data using Eq. (12).

is completely bound to the micelle during the quenching process, then the relationship between fluorescence intensity and quencher concentration is [30]

$$\frac{F}{F_0} = \exp\left(-\frac{K[\mathrm{Q}]}{1+K[\mathrm{M}]}\right), \tag{11}$$

where [M] is the micelle concentration and K is the ratio of rate constants for quencher entry and exit of the micelle (i.e. k_+/k_-). Unfortunately, this model gave the poorest fits to the data. An example is shown in Fig. 5, where a fit of the B(a)P/TX-100/I^- system was attempted. The chi-squared value for the fit was 0.05. This model may be inappropriate here because one assumes that every micelle occupied by both a probe and quencher results in fluorescence quenching. This may not be true for the systems studied in the present work.

The B(a)P/SDS/I^- system defied both the simple and modified Stern–Volmer approaches by increasing efficiency with quencher concentration, apparently in an exponential fashion. For this situation, often the case of combined static and dynamic quenching applies. This approach did not model the experimental data satisfactorily. Instead a modified model based on a simple Stern–Volmer equation was applied. The empirical model that fits the data was

$$\frac{F_0}{F} = 1 + K''_{\mathrm{SV}}[\mathrm{Q}]^a. \tag{12}$$

The best fit was produced setting a=3. The data and the fit are presented in Fig. 6. The definition of K''_{SV} will be treated in the next section. Its value is 2.5(±1) M^{-3}.

4. Discussion

With the exception of the PRODAN/TX-100 system, it seems unlikely that the quenching saturation observed is due to an inaccessible fraction of probe. This is because there is no spectral evidence for multiple probe locations. If there were different locations for these probes within the micelles, then the fluorescence spectra should broaden compared with pure solution [28,31]. We see no broadening effect for B(a)P or for PRODAN in systems other than PRODAN/TX-100. However, a shifting of the fluorescence maxima is observed for each micelle system. The difference in the fluorescence spectra between TX-100 and SDS micelle solution for both probes is due to solvatochromic effects. For PRODAN, the SDS micelle environment is similar to methanol ($\lambda_{\max}$=510 nm). Since B(a)P should not develop an appreciable electric dipole moment in its excited state, there will be little shifting in the energy of its lowest excited state between surfactant systems. The measured difference between SDS and TX-100 for B(a)P fluorescence can be accounted for via dispersive interactions [31]. Thus, the red shift in TX-100 micelles (cf. SDS) is due to the larger polarizability of the aromatic system of B(a)P. For both micelle systems, B(a)P senses an environment which has electric properties similar to toluene.

The fluorescence spectra provide clues to the positions of the probes within the micelles. Knowing these positions will be important in the interpretation of the quenching results. The spectrum of PRODAN in SDS micelle solution has been previously reported [25,28]. From the maximum of the fluorescence spectrum and its amphiphilic nature, it is likely that PRODAN exists near, but not on, the surface of the SDS micelle. The location of PRODAN in TX-100 micelles should be between the surface and somewhere deeper in the polyethylene-oxide (PEO) region. The extreme hydrophobicity of B(a)P suggests that it would partition deep within a micelle. In SDS, the B(a)P fluorescence maximum is suggestive of a nonpolar, but polarizable medium. This will exist in the high-density alkane SDS micelle center. In TX-100 micelles, B(a)P will be located nearer to the aromatic system, but removed from the PEO annulus. This environment is found in the center of the micelle. This is consistent with other spectral studies, which suggest that

pyrene can also be found in the center (alkane region) of TX-100 micelles [32,33].

Recall the saturation isotherms presented in Fig. 4a–d. The first notable trend is that the saturation equations (i.e. Eqs. (3) and (10)) represent very successful fits to the data in four distinct cases. These cases are those where the quenching is proceeding in TX-100 micelle solution for B(a)P and PRODAN. This suggests that there is a unique type of quenching site for these micelles.

We will first consider the PRODAN/TX-100 system and compare the iodide and peroxide quenching mechanisms. From Table 1 we see that the fraction of accessible quencher is much greater for I^- than for H_2O_2 quenching (0.68 versus 0.15). Since the difference spectra suggest that the fraction quenched is at the same micelle location, the difference in accessibility must come from the quencher. This could simply result from the requirement that H_2O_2 must be closer to PRODAN for quenching to occur. This would be true if the H_2O_2 quenched fluorescence via a short-range electron transfer mechanism, whereas I^- would quench fluorescence via the heavy atom effect. The Stern–Volmer constant for H_2O_2 is more than twice that for I^-. This again could result from the H_2O_2 needing a closer approach in order to quench fluorescence, but being a more efficient quencher upon those close encounters.

In Fig. 7 we present a cartoon of the possible PRODAN locations in a TX-100 micelle. The more red-shifted fluorescence (490 nm) would arise from the surface fraction and the blue fluorescence from the more deeply buried fraction (470 nm) near the aromatic/polyethylene-oxide interface. It is likely that the micelle surface fraction is being quenched. This suggests that the quenchers need not actually penetrate the micelle. Thus, the fraction of quenching encounters are lower for H_2O_2 because of the lower fraction of close approaches compared with the longer distance I^- quenching mechanism.

We will now examine the B(a)P/TX-100 system. Here the saturation of quenching has been modeled using Eq. (10), because we observed no spectral evidence for an inaccessible fraction of B(a)P. The values for K'_{SV} follow a trend associated with the type of quencher. The K'_{SV} constants for iodide are greater than that for peroxide. This trend makes sense if the iodide does not require as close an approach as peroxide does. I^- may have more active occupation sites for quenching of B(a)P. Alternatively, the value of K_{SV} may be larger for B(a)P/I^-, but again this would potentially lead to a greater number of quenching sites. The K_Q for B(a)P in TX-100 for I^- versus H_2O_2 is greater by almost a factor of 5. This suggests that the on/off kinetics for quenching-site occupation by H_2O_2 and I^- are different and that there is greater penetration of the micelle by I^-.

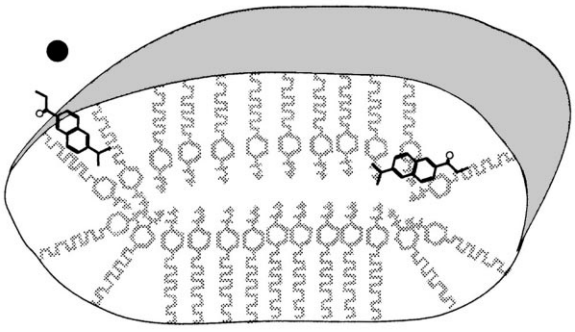

Fig. 7. A schematic representation of a slice through a Triton X-100 micelle. PRODAN has two locations. One is at the micelle–solution interface and the other is at interfacial region between the aromatic moiety and the polar polyethylene-oxide region. The dot represents I^-.

Comparing the B(a)P/TX-100/I^- versus PRODAN/TX-100/I^- systems one finds that the quenching efficiency is greater for B(a)P. Since the quencher and micelle are the same, this result can be explained only through an effect of the fluorophore. We have shown that neither PRODAN nor B(a)P affect the cmc for TX-100 [28]. Therefore, there must be unique quenching sites for these two micelle-bound fluorophores. Apparently for iodide, the quenching site of B(a)P is more easily accessed. The fit of the PRODAN/TX-100/I^- system to Eq. (3) suggests that the accessible fraction is about 67%. Since B(a)P only has one location and is quenched more efficiently by I^-, there must be more operative I^- quenching sites in this case. Interestingly, the converse is true for H_2O_2 quenching of these two fluorophores in TX-100 solution, although the difference is smaller. Thus, the deeply buried B(a)P/TX-100 site is less easily accessed by H_2O_2.

We will now turn to the SDS micelle system, which is less well modeled than TX-100. The two systems which appear to follow the saturation model for SDS are PRODAN with either quencher. Although, it is arguable that a standard Stern–Volmer approach works nearly as well. The chi-squared values for the saturation isotherm fits are slightly better than for the linear Stern–Volmer fits (0.0004 versus 0.001), but there is considerably more scatter in the data than for the TX-100 system. Therefore, a detailed discussion of the saturation isotherm parameter values may be misleading. We will consider only generalities.

The complex behavior of quenching fluorophores in SDS micelles may have several origins. The first is that at high ionic strength, SDS micelles have been observed to display bimodal size distributions [9]. This means that there may also be a distribution of several different quenching sites. This is not accounted for in our simple saturation isotherm model. The second possibility is that the quenching mechanism itself may be different for SDS micelle solutions. This would be particularly true of anionic quenchers such as I^-, which would have to pay an extraordinary free energy toll to cross the surface of an SDS micelle. In fact, we suggest that, at least for B(a)P in SDS, the quencher is actually I_3^-. Finally, the smaller average size of SDS micelles compared with TX-100 (hydrodynamic radii of 21 Å versus 43 Å) [33,34] may lead to different quenching behavior. The size effect may result in some quench-

ing taking place without quencher partitioning into the SDS micelle.

The anomalous case of the B(a)P/SDS/I^- system is worthy of contemplation. From Fig. 6, it is apparent that this system does not display the saturation behavior observed in the other systems presented. The exponential increase in quenching efficiency is also observed in SDS solution with micelle concentration of 10 mM. Thus, we conclude that this is not an effect due to the surfactant. We propose that the exponential iodide concentration dependence results either from the formation of I_3^- ions in solution or from the formation of I_3^- ions in solution followed by the partitioning of I_2 into the SDS micelles. The chemical reactions would involve an oxidation of I^- by water to form I_3^-:

$$3I^-(aq) + 2H_2O \Leftrightarrow I_3^-(aq) + 2OH^-(aq) + 2H_2(g) \quad (13)$$

This reaction is thermodynamically spontaneous under the experimental conditions used. Thus, if I_3^- was the species that quenches B(a)P in SDS, the quenching of B(a)P in NaI solution would depend on the third power of the iodide ion concentration. Eq. (13) allows us to define the quenching constant, K''_{SV}, from Eq. (12).

$$K''_{SV} = \frac{K_{SV}K}{[OH^-]^2(pH_2)^2}, \quad (14)$$

where K is the equilibrium constant for Eq. (13). Unfortunately, we cannot use this to determine K_{SV} directly for two reasons. The first is that we do not know the partial pressure of H_2 evolved. The second is that we are not working under standard electrochemical conditions and therefore cannot predict the exact value of K. Nevertheless, we can suggest that the value of K_{SV} is less than that of K''_{SV}. This is because the equilibrium constant, K, should be greater than 1, the value of $[OH^-]$ is less than 1 M according to our buffer conditions and the value of pH_2 should be less than 1 atm. Thus, the value of $K_{SV} < 2.5\,M^{-1}$.

If the B(a)P/SDS/I^- system is truly different from the others then there may be some spectral evidence of this. There are features in the absorbance spectrum for this system that suggest the presence of I_3^-. The absorbance spectrum of this system is presented in Fig. 8. There is a feature, which peaks around 350 nm, that increases with increasing iodide concentration. The feature is obtained by subtracting the quencher free B(a)P spectrum from that with iodide present. The feature follows an $[I_3^-]$ intensity dependence and possesses the appropriate λ_{max} to be tri-iodide in aqueous solution [35]. Using the previously determined value for the molar absorption coefficient (25,750 M^{-1}) [36], the concentration of tri-iodide is calculated to be 3 μM.

Any possible mechanism for the quenching of B(a)P in SDS micelles by I_3^- should be unique to the B(a)P/SDS/I^- system. Resonance energy transfer (RET) is a distinct possibility here. We use RET instead of fluorescence resonance energy transfer (FRET), because the acceptor, I_3^- does not fluorescence appreciably. Note from Fig. 8 that there is considerable overlap between the red tail of the I_3^- absorbance

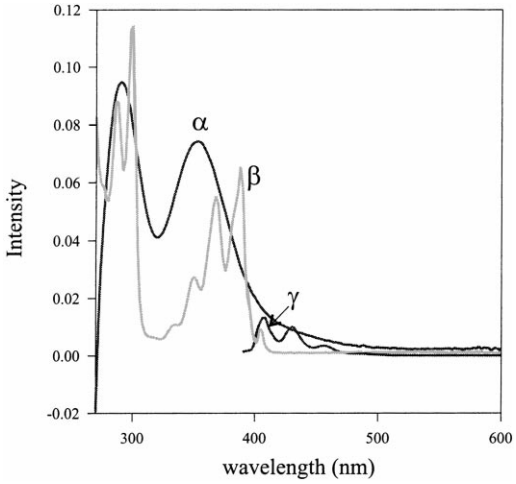

Fig. 8. The absorbance spectra of I_3^- in 1 μM benzo(a)pyrene, α, 80 mM SDS, 0.4 M NaI solution and benzo(a)pyrene, β, in 1 μM benzo(a)pyrene, 80 mM SDS solution. Also shown is the fluorescence spectrum of B(a)P, γ, resulting from excitation at 380 nm of the above solution without NaI present. The I_3^- spectrum was obtained by subtracting the NaI free B(a)P absorbance spectrum from that containing 0.4 mM NaI.

spectrum and the fluorescence spectrum of B(a)P. Such an overlap does not exist between PRODAN and I_3^-. Generally for RET the fluorescence donor and acceptor must be within 100 Å of each other. Given the concentrations of SDS and I_3^-, the average micelle–micelle and I_3^-–I_3^- distances would be 75 and 535 Å, respectively. Since, in solution, the SDS micelles will be dispersed between the I_3^- ions, the micelle–I_3^- distance will be between 75 and 270 Å. From space filling arguments, the average distance is 113 Å. Using this distance, R_0 for RET can be estimated from the quenching efficiency [37]. We find a quenching efficiency of 10%. This produces an R_0 of 78 Å, which is a rather large value, but not totally unreasonable considering the extensive donor–acceptor spectral overlap.

We can further rationalize I_3^- as the main source of quenching in the B(a)P/SDS/F system with the following argument. Since there is considerable coulombic repulsion between the negatively charged quenchers (I^- or I_3^-) and the SDS micelle, there is little chance of quencher penetration into the micelle. Thus, RET is the only possible quenching mechanism operative at the extended distances of 100 Å necessary for B(a)P(SDS)–I_3^-(aq) interactions. This eliminates I^- as the quencher for this system. Although I_3^- is also present in the B(a)P/TX-100/I^- system, the fact that I^- can penetrate the micelle at least somewhat [34,38], coupled with its overwhelming concentration (13,000 times that of tri-iodide) makes I^- the operative quencher.

5. Conclusions

Saturation in probe fluorescence quenching efficiency was observed for the TX-100 system using high concentrations

(0.1–0.4 M) of both I^- and H_2O_2. These data were modeled quite well using a modified linear Stern–Volmer equation with a limited number of quenching sites per micelle. For B(a)P this is different from previous models in that a distinction is made here between quencher binding sites on the micelle and binding sites which actually result in fluorescence quenching. For the SDS system, similar quenching saturation effects were observed, but the saturation model worked less well. This is possibly due to a bimodal distribution of micelle sizes. The B(a)P/SDS/I^- system is surprising in that the quenching does not saturate. The efficiency of quenching here varies approximately with the third power of I^- concentration. A RET mechanism is proposed whereby micelle-bound B(a)P is quenched by free I_3^-.

Acknowledgements

This work is supported by the Natural Sciences and Engineering Research Council of Canada. Financial assistance from the University of Calgary is also gratefully appreciated. The authors are indebted to Professors G. Liu and C.H. Langford (University of Calgary) for the use of their spectrometers and to Professor D.A. Armstrong for valuable discussions.

References

[1] R.S. Sarpal, S.K. Dogra, J. Photochem. Photobiol. A 88 (1995) 147.
[2] S.C. Bhattacharya, H.T. Das, S.P. Moulik, J. Photochem. Photobiol. A 81 (1993) 257.
[3] H. Huang, R.E. Verrall, B. Skalski, Langmuir 13 (1997) 4821.
[4] S.S. Atik, L.A. Singer, Chem. Phys. Lett. 59 (1978) 19.
[5] H.W. Ziemiecki, R. Holland, W.R. Cherry, Chem. Phys. Lett. 73 (1980) 145.
[6] S.K. Saha, G. Krishnamoorthy, S.K. Dogra, J. Photochem. Photobiol. A 121 (1999) 191.
[7] R.G. Alatgova, I.I. Kochijashky, M.L. Sierra, R. Zana, Langmuir 14 (1998) 5412.
[8] A.P. Rodenheiser, J.C.T. Kwak, J. Phys. Chem. B 103 (1999) 2970.
[9] A. Siemiarczuk, W.R. Ware, W. Dong, J. Fluoresc. 7 (1997) 1955.
[10] A.S. Varela, M.I.S. Macho, A.G. Gonzalez, Colloid Polym. Sci. 273 (1995) 876.
[11] P. Ray, S.C. Bhattacharya, S.P. Moulik, J. Photochem. Photobiol. A 116 (1998) 85.
[12] M.H. Gehlen, Chem. Phys. 224 (1997) 275.
[13] Y. Umebayashi, M. Shin, S. Ishiguro, J. Colloid Int. Sci. 191 (1997) 391.
[14] M.E. Dario, P.F. Aramendia, E. San Roman, Chem. Phys. Lett. 250 (1996) 203.
[15] S. Carrigan, S. Doucette, C. Jones, C.J. Marzzacco, A.M. Halpern, J. Photochem. Photobiol. A 99 (1996) 29.
[16] M. Mac, J. Najbar, J. Wirz, Chem. Phys. Lett. 235 (1995) 187.
[17] M.C. Gehlen, F.C. De Schryver, J. Phys. Chem. 97 (1993) 11242.
[18] T. Nakamura, A. Kira, M. Imamura, J. Phys. Chem. 87 (1983) 3122.
[19] O. Stern, M. Volmer, Phys. Z. 20 (1919) 18.
[20] S.S. Lehrer, Biochemistry 10 (1971) 3254.
[21] M. Maruthamuthu, G. Selbakumar, Proc. Indian Acad. Sci. 107 (1995) 79.
[22] C.L. Wambolt, S.S. Saavedra, J. Sol–Gel Sci. Technol. 7 (1996) 53.
[23] M. Tachiya, in: G.R. Freeman (Ed.), Kinetics of Nonhomogeneous Processes, Wiley, New York, 1987, p. 575.
[24] A.V. Barzykin, M. Tachiya, J. Phys. Chem. B 102 (1998) 1296.
[25] K.K. Karukstis, S.W. Suljak, P.J. Waller, J.A. Whiles, E.H.Z. Thompson, J. Phys. Chem. 100 (1996) 11125.
[26] J.L. Vazquez, M.T. Montero, J. Trias, J. Hernandez-Borrell, Int. J. Pharm. 171 (1998) 75.
[27] A.W. Adamson, Physical Chemistry of Surfaces, Wiley, New York, 1990.
[28] J. Wong, T.M. Duchscherer, G. Peitraru, D.T. Cramb, Langmuir 15 (1999) 6181.
[29] E. Blatt, R.C. Chatelier, W.H. Sawyer, Chem. Phys. Lett. 108 (1984) 397.
[30] M.H. Gehlen, F.C. DeSchryver, Chem. Rev. 93 (1993) 199.
[31] S.C. Beck, D.T. Cramb, J. Phys. Chem., 2000, in press.
[32] E.A. Cummings, T.T. Ndou, V.K. Smith, I.M. Warner, Appl. Spectrosc. 47 (1993) 2129.
[33] F.G. Sanchez, C.C. Ruiz, J. Luminesc. 55 (1993) 321.
[34] N.C. Maiti, M.M.H.G. Krishna, P.J. Britto, N. Periasamy, J. Phys. Chem. B 101 (1997) 11051.
[35] T. Okada, J. Hata, J. Mol. Phys. 43 (1981) 1151.
[36] D.A. Palmer, R.W. Ramette, R.E. Mesmer, J. Sol. Chem. 13 (1984) 673.
[37] J.R. Lakowicz, Principles of Fluorescence Spectroscopy, Plenum Press, New York, 1983.
[38] F. Moro, F.M. Goni, M.A. Urbaneja, FEBS Lett. 330 (1993) 129.